

# Critical Casimir forces in colloidal suspensions on chemically patterned surfaces

Florian Soyka,<sup>1</sup> Olga Zvyagolskaya,<sup>1</sup> Christopher Hertlein,<sup>1</sup> Laurent Helden,<sup>1</sup> and Clemens Bechinger<sup>1,2</sup>

<sup>1</sup>*2. Physikalisches Institut, Universität Stuttgart, Pfaffenwaldring 57, 70550 Stuttgart, Germany*

<sup>2</sup>*Max-Planck-Institut für Metallforschung, Heisenbergstr.3, 70569 Stuttgart, Germany*

We investigate the behavior of colloidal particles immersed in a binary liquid mixture of water and 2,6-lutidine in the presence of a chemically patterned substrate. Close to the critical point of the mixture, the particles are subjected to critical Casimir interactions with force components normal and parallel to the surface. Because the strength and sign of these interactions can be tuned by variations in the surface properties and the mixtures temperature, critical Casimir forces allow the formation of highly ordered monolayers but also extend the use of colloids as model systems.

PACS numbers: 82.70.Dd, 68.35.Rh, 81.16.Dn

Analogous to the geometrical confinement of quantum-electrodynamical (QED) vacuum fluctuations between two parallel metallic plates [1], the constraint of concentration fluctuations in fluid mixtures close to their critical point gives rise to critical Casimir forces acting on the confining surfaces [2]. The range of this interaction is set by the bulk correlation length  $\xi$  of the mixture which diverges when approaching the critical point. Therefore, critical Casimir forces are sensitive to minute changes in temperature. Despite several quantitative measurements of such forces [3, 4], it was only recently when the amplitude of measured critical Casimir forces in quantum- and classical liquids has been directly compared to theoretical predictions [5, 6, 7, 8]. Direct force measurements of a single colloidal particle above a flat surface and immersed in a critical water-lutidine mixture demonstrated, that critical Casimir interactions can easily exceed multiples of the thermal energy  $k_B T$  [8]. Accordingly, they offer a versatile opportunity to control the pair interaction in colloidal suspensions by weak temperature changes [9, 10]. Apart from their exquisite temperature dependence, critical Casimir forces respond sensitively to the chemical properties of the confining surfaces. Depending on whether both surfaces preferentially attract the same mixture's component or not (symmetric or asymmetric boundary conditions), attractive or repulsive critical Casimir forces arise [8, 11, 12].

So far, experimental investigations of critical Casimir interactions were limited to homogeneous surfaces (in contrast to QED Casimir forces [13]) where the corresponding forces act perpendicular to the confining walls. However, when one or both surfaces are chemically patterned, also lateral critical Casimir forces have been predicted [14]

In this Letter we experimentally study the interaction between colloidal particles and chemically patterned substrates immersed in a binary critical mixture. Close to the critical point lateral critical Casimir forces lead to the formation of highly ordered colloidal assemblies whose structure is controlled by the underlying chemical pattern. This may suggest a novel route for templated growth of colloidal crystals. At higher particle concentra-

tions, additional critical Casimir forces between nearby particle surfaces arise and eventually lead to the formation of three-dimensional, faceted colloidal islands on the substrate. Because the particle-substrate and the particle-particle critical Casimir interactions can be systematically and independently varied, this also leads to new opportunities in the use of colloidal model systems to study the growth of islands on surfaces as this is important for the fabrication of nanostructures [15].

We used  $2.4 \mu\text{m}$  diameter polystyrene (PS) spheres with a surface charge of  $10 \mu\text{C}/\text{cm}^2$  rendering them hydrophilic which corresponds to  $(-)$  boundary conditions [16]. They were suspended in a water-2,6-lutidine (WL) mixture with critical composition, i.e. a lutidine mass fraction of  $c_L^C \cong 0.286$  [17]. WL mixtures have a lower critical demixing point at  $T_C \cong 307 \text{K}$  [17]. The Debye screening length of the mixture was determined with total internal reflection microscopy (TIRM) to  $\kappa^{-1} \cong 12 \text{nm}$  from the particle-wall interaction potential between a single colloidal sphere and a flat glass surface [8]. The suspension was contained in a flat sample cell being assembled from a glass substrate, a  $150 \mu\text{m}$  thick spacer and a glass cover plate with two filling tubes.

To fabricate glass surfaces with well defined spatial variations regarding their boundary conditions, they have been first coated with a monolayer hexamethyldisilazane (HMDS). This was achieved by exposure to its saturated vapor for several hours in an exicator [8]. This treatment renders the glass surface hydrophobic with preferential adsorption for lutidine, i.e.  $(+)$  boundary condition as confirmed by previous TIRM measurements. Spatial patterning of the boundary conditions was achieved by exposure of HMDS coated surfaces to a focussed ion beam (FIB) of positively charged gallium (Ga) ions. The incident ions locally remove the HMDS molecules from the surface and thus create well-defined hydrophilic  $(-)$  areas. To avoid possible distortion of the ion beam due to charging effects of the isolating glass surface, the latter was simultaneously exposed to an electron beam. With this procedure we created chemical patterns with a lateral resolution on the order of several tens of nanometers extending over an area of approx.  $400 \times 400 \mu\text{m}^2$ . Typical

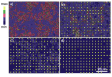


FIG. 1: (color online) Averaged particle density distribution  $\rho(x, y)$  of a diluted colloidal suspension of  $2.4 \mu\text{m}$  particles in a critical water-lutidine mixture in the presence of a chemically patterned substrate.  $T_c - T = 0.72 \text{ K}$  (a),  $0.25 \text{ K}$  (b),  $0.23 \text{ K}$  (c), and  $0.14 \text{ K}$  (d).

parameters for the current, voltage and dose of the Ga ions were on the order of  $1 \text{ nA}$ ,  $30 \text{ kV}$  and  $26 \mu\text{C}/\text{cm}^2$ . For the electron beam similar currents but only voltages on the order of  $5 \text{ kV}$  were used. After the substrate patterning, the cell was assembled and the suspension was inserted. Finally, the filling tubes were sealed with teflon plugs to avoid evaporation of the mixture. The upper part of the sample cell was thermally connected to a copper frame (having a window to allow for optical access) and connected to a flow thermostat which provided a constant temperature  $1 \text{ K}$  below  $T_C$  with a stability of  $0.01 \text{ K}$ . For precise temperature control, the cell was actively heated from below with a transparent indium tin oxide (ITO) coated glass sheet which was operated by a temperature controller. As thermometers we used two platinum resistors (Pt100) which were contacted from outside to the sample cell. With this setup we achieved a temperature stability of about  $10 \text{ mK}$  over several hours. The entire sample and heating unit was mounted on the stage of an inverted microscope where particle positions were determined by digital video microscopy with a spatial resolution of about  $50 \text{ nm}$  [18].

Fig. 1 shows the two-dimensional particle distribution  $\rho(x, y)$  of highly diluted colloidal suspension in a WL-mixture above a chemically patterned substrate. As substrate pattern we have chosen squares with  $(-)$  boundary conditions and  $2.6 \mu\text{m}$  side length arranged in a square lattice with  $5.2 \mu\text{m}$  periodicity. For temperatures  $T_C - T = 0.72 \text{ K}$  where critical Casimir forces are negligible [8], the colloidal particles do not respond to the substrate pattern but are rather evenly distributed across the field of view (Fig. 1a). This demonstrates that possible lateral variations of the van-der-Waals [14] or electrostatic interactions caused by the FIB treatment can be neglected under our experimental conditions. Upon approaching  $T_C$ , the PS particles become increasingly lo-

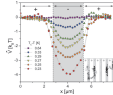


FIG. 2: (color online) Temperature-dependent critical Casimir potential acting on a hydrophilic  $2.4 \mu\text{m}$  PS particle above a chemically striped pattern with alternating  $(-)$  and  $(+)$  boundary conditions. Line widths are  $2.6 \mu\text{m}$   $(-)$  and  $5.2 \mu\text{m}$   $(+)$ , respectively. Inset: trajectories of two particles recorded over  $45 \text{ min.}$  on striped chemically patterned substrate with  $(-)$  regions indicated in grey.

calized at the hydrophilic squares while they avoid the hydrophobic regions as seen in Figs. 1b-d. This behavior is due to gradient forces caused by critical Casimir interactions which lead to a strongly temperature dependent attraction of the  $(-)$  PS particles at the hydrophilic squares (symmetric boundary conditions) and a repulsion from the hydrophobic regions  $(+)$  (asymmetric boundary conditions). Because the particle size is similar to that of the chemical substrate pattern,  $\rho(x, y)$  eventually resembles the geometry of the underlying substrate pattern as seen in Fig. 1d.

To quantify lateral critical Casimir forces, we created substrates having a one-dimensional periodic chemical pattern, i.e. hydrophilic  $(-)$  and hydrophobic  $(+)$  stripes with  $2.6 \mu\text{m}$  and  $5.2 \mu\text{m}$  width, respectively. Similar as above, the PS colloids are strongly confined to the  $(-)$  stripes when the WL-mixture is heated close to  $T_C$  as seen by the asymmetric shape of the particle trajectories (inset of Fig. 2). The critical Casimir potential  $V(x, y, z)$  of a particle above a patterned substrate depends on its lateral position  $x, y$  and height  $z$  above the surface. Since the  $z$ -coordinate is not accessible with digital video microscopy, the measured  $\rho(x, y)$  corresponds to the projection of the three-dimensional particle distribution onto the  $xy$ -plane. For the one-dimensional surface pattern as considered here, these data can be further projected onto the  $x$ -axis (being perpendicular to the direction of the stripes). From the resulting one-dimensional particle distribution  $\hat{\rho}(x)$  we define the effective one-dimensional

critical Casimir potential via the Boltzmann factor

$$\frac{\hat{V}(x)}{k_B T} = -\ln \hat{\rho}(x) + c \quad (1)$$

with  $c$  an arbitrary constant. In Fig. 2 we show the results for a single period as a function of temperature. It is clearly seen that upon approaching  $T_C$ , the critical Casimir potential becomes increasingly attractive at the stripes with  $(-)$  boundary condition. The measured nonlinear temperature dependence of the potential depth  $\Delta\hat{V}$  is shown in Fig. 3 as closed symbols. We have limited these measurements to temperatures where  $\Delta\hat{V} < 4 k_B T$  to allow for occasional particle escapes from the potential wells during the measuring time which are required to sample the entire energy landscape. It should be mentioned, however, that much deeper potentials can be obtained by further approaching  $T_C$ .

For a quantitative estimate, we assumed that  $\Delta\hat{V}$  is given by

$$\Delta\hat{V} \cong V_{(-)} - V_{(+)} \quad (2)$$

where  $V_{(-)}$  and  $V_{(+)}$  are the critical Casimir potentials of the colloid above infinite homogeneous substrates with  $(-)$  and  $(+)$  boundary condition, respectively. These potentials only depend on the corresponding particle heights  $z_{(-)}$  and  $z_{(+)}$ . Although Eq. (2) ignores the finite width of the stripes (which is only slightly larger than the particle diameter), this simplification is justified here as can be seen by the almost vanishing curvature of  $\hat{V}(x)$  near its minimum. The critical Casimir potential of a colloidal sphere with radius  $R$  at height  $z$  above a homogeneous surface is given by [8]

$$\frac{V}{k_B T} = \frac{R}{z} \vartheta \left( \frac{z}{\xi} \right) \quad (3)$$

with  $\vartheta$  the corresponding universal scaling function for symmetric and asymmetric boundary condition which have been inferred from recent Monte Carlo simulations for classical binary mixtures [8, 19]. The correlation length is given by  $\xi = \xi_0 \left( \frac{T_C - T}{T_C} \right)^{-0.63}$  with  $\xi_0 \approx 0.2 \mu\text{m}$  for water-lutidine mixtures as determined experimentally [8, 20]. What remains for the calculation of  $\Delta\hat{V}$  from Eqs.(2) and (3) are the temperature-dependent particle heights of a  $2.4 \mu\text{m}$  PS particle on a substrate with  $(-)$  and  $(+)$  boundary condition. The height distributions have been measured with TIRM with an accuracy of  $\pm 30 \text{ nm}$  and yield temperature-dependent mean values of  $\langle z \rangle_{(-)} = 0.12 \mu\text{m}$  and  $0.11 \mu\text{m} \leq \langle z \rangle_{(+)} \leq 0.2 \mu\text{m}$ . Note, that within our experimental resolution,  $\langle z \rangle_{(-)}$  does not vary with temperature due to the strong electrostatic repulsion at small distances. The calculated temperature-dependence of  $\Delta\hat{V}$  is shown as open symbols in Fig. 3. Best agreement with the experimental data is obtained when assuming that  $T_C$  is 80 mK lower than the



FIG. 3: (color online) Temperature dependence of measured (closed symbols) and calculated (open symbols) potential depth of a  $2.4 \mu\text{m}$  PS particle on a substrate with one-dimensional, periodic alternating boundary conditions. The critical temperature has shifted by 80 mK within our experimental accuracy to obtain best agreement with the experimental data. The dashed line is a guide to the eye.

temperature where the onset of phase separation (being identified as  $T_C$ ) has been experimentally observed. This shift is within our error in determining the critical temperature with this procedure. The good agreement in Fig. 3 also confirms that the above assumption (Eq. (2)) is indeed reasonable under our conditions.

When further increasing the particle density, critical concentration fluctuations become also confined between adjacent colloidal surfaces. This leads - in addition to the forces between the particles and the substrate - to critical Casimir interactions between adjacent particles. Within the Derjaguin approximation its amplitude is one-half of Eq. (3) [21]. To study the interplay of those forces we created a substrate with a single chemical step, i.e. with  $(-)$  boundary conditions on the left and  $(+)$  on the right side. As can be seen in Fig. 4 the colloidal particles in a critical water-lutidine mixture form rather different structures on each side of the substrate. On the left side, all boundary conditions (particle-particle and particle-substrate) are symmetric  $(--)$  thus leading to attractive interactions. Upon approaching the critical temperature, this leads essentially to a loosely-packed single layer of particles as seen on the left side of Fig. 4a. Because of vertical particle fluctuations, some colloids (appearing as bright spots) are initially located on top of this layer when increasing the temperature towards  $T_C$ . However, when keeping the system at constant temperature, most of these particles laterally diffuse until they reach a void where they merge into the first layer (Fig. 4b, left).

The situation on the hydrophobic part of the sample (right side of Fig. 4a) is different, because here the parti-

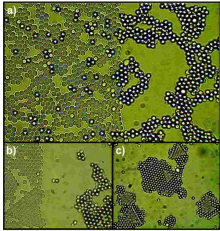


FIG. 4: (color online) (a) Snapshot of a colloidal suspension above a substrate with a chemical step, i.e.  $(-)$  and  $(+)$  boundary conditions at the left and right part of the sample. Due to attractive (left) and repulsive (right) critical Casimir forces between the particles and the substrate, a monolayer forms on the left while at the right side the particles arrange in three-dimensional clusters. (b) Detail of the region at the chemical interface after the system was kept for several hours at constant temperature. (c) Optical image of the faceted islands which form on the hydrophobic substrate when the sample is kept for several hours at constant temperature.

cles are repelled from the substrate ( $(+-)$  boundary conditions). When approaching the critical temperature, the particles initially form a three-dimensional rather open structure. At larger timescales and constant temperature, however, the clusters rearrange and eventually form faceted close-packed islands with heights up to three particle diameters (Fig. 4c). At very large timescales (several hours) even the aggregation of entire clusters has been observed. We expect that for other parameters where the critical Casimir interaction energy largely exceeds  $k_B T$ , surface diffusion of particles becomes reduced. Accordingly, this should then lead to fractal or dendritic structures.

To conclude, we have reported on the use of critical Casimir forces as a novel and robust approach for colloidal assembly on chemically patterned surfaces. Since these forces can be controlled by variations in the surface properties and the mixtures temperature, critical Casimir forces lead to a rich phase behavior. In contrast to other aggregation mechanisms, critical Casimir forces are fully reversible which allows to thermally anneal the obtained structures. This will result in a largely reduced defect density being important for technical ap-

plications [22][23]. Since critical Casimir forces are not restricted to micron-sized particles, the principle as discussed here should be also applicable on smaller length scales. It should be also mentioned that chemical patterns can be obtained by other techniques than a FIB, e.g. by self-assembled monolayers deposited on gold-coated substrates with microcontact-printing [24].

We thank U. Eigenthaler, A. Breitling and M. Hirscher for technical assistance during creation of chemical substrate patterning with the FIB, U. Nellen for TIRM measurements and A. Gambassi, L. Harnau and S. Dietrich for helpful discussions.

- 
- [1] H. B. G. Casimir, Proc. Kon. Nederl. Akad. Wet **B51**, 793 (1948).
  - [2] M. E. Fischer, and P. G. de Gennes, C. R. Acad. Sci. paris **B287**, 207 (1978).
  - [3] A. Mukhopadhyay, and B. M. Law, Phys. Rev. Lett. **83**, 772 (1999).
  - [4] S. Rafai, D. Bonn, and J. Meunier, Physica A **386**, 31 (2007).
  - [5] R. Garcia, and M. H. W. Chan, Phys. Rev. Lett. **83**, 1187 (1999).
  - [6] A. Ganshin, S. Scheidemantel, R. Garcia, and M. H. W. Chan, Phys. Rev. Lett. **97**, 075301 (2006).
  - [7] M. Fukuto, Y. F. Yano, and P. S. Pershan, Phys. Rev. Lett. **94**, 135702 (2005).
  - [8] C. Hertlein, L. Helden, A. Gambassi, S. Dietrich, and C. Bechinger, Nature **451**, 172 (2008).
  - [9] H. Guo, T. Narayanan, M. Sztuchi, P. Schall, and G. H. Wegdam, Phys. Rev. Lett. **100**, 188303 (2008).
  - [10] X. H. Lu, S. G. J. Mochrie, S. Narayanan, A. R. Sandy, and M. Sprung, Phys. Rev. Lett. **100**, 045701 (2008).
  - [11] M. Krech, Phys. Rev. E **56**, 1642 (1997).
  - [12] T. W. Burkhardt, and E. Eisenriegler, Phys. Rev. Lett. **74**, 3189 (1995).
  - [13] F. Chen, U. Mohideen, G.L. Klimchitskaya, and V.M. Mostepanenko, Phys. Rev. Lett. **88**, 101801 (2002).
  - [14] M. Sprenger, F. Schlesener, and S. Dietrich, J. Chem. Phys. **124**, 134703 (2006).
  - [15] J. V. Barth, G. Costantini, and K. Kern, Nature **437**, 671 (2005).
  - [16] P. D. Gallagher, M. L. Kurnaz, and J. V. Maher, Phys. Rev. A **46**, 7750 (1992).
  - [17] D. Beysens, and D. Esteve, Phys. Rev. Lett. **54**, 2123 (1985).
  - [18] J. Baumgartl, and C. Bechinger, Europhys. Lett. **71**, 487 (2005).
  - [19] O. Vasilyev, A. Gambassi, A. Maciolek, and S. Dietrich Europhys. Lett. **80**, 60009 (2007).
  - [20] E. Güleri, A. F. Collings, and R. L. Schmidt, J. Chem. Phys. **56**, 6169 (1972).
  - [21] F. Schlesener, A. Hanke, and S. Dietrich, J. Stat. Phys. **110**, 981 (2003).
  - [22] O. D. Velev, and E. W. Kaler, Langmuir **15**, 3693 (1999).
  - [23] A. Albrecht, G. Hu, I. L. Guhr, T. C. Ulbrich, J. Boneberg, P. Leiderer, and G. Schatz, Nature Materials **4**, 203 (2005).
  - [24] A. Kumar, and G. M. Whitesides, Appl. Phys. Lett. **63**,

2002 (1993).